ELSEVIER

Polymer 44 (2003) 2049–2055

polymer

www.elsevier.com/locate/polymer

Conformation in solution of side-chain liquid crystal polymers as a function of the mesogen-graft amount

David Rousseau[a], Jean-Daniel Marty[b], Monique Mauzac[b], Philippe Martinoty[a,*], Astrid Brandt[c], Jean-Michel Guenet[d]

[a]*Laboratoire de Dynamique des Fluides Complexes, CNRS-ULP UMR 7506, 4, rue Blaise Pascal, F-67070 Strasbourg Cedex, France*
[b]*Laboratoire des Interactions Moléculaires et Réactivité Chimique et Photochimique, U.M.R. CNRS 5623, Université Paul Sabatier, 118 Route de Narbonne, F-31062 Toulouse Cedex 4, France*
[c]*Hahn-Meitner Institut, BENSC, Glienicker Strasse 100, D-14109 Berlin, Germany*
[d]*Institut Charles Sadron CNRS UPR 22, 6, rue Boussingault, F-67083 Strasbourg Cedex, France*

Received 9 July 2002; received in revised form 27 December 2002; accepted 14 January 2003

Abstract

The conformation of side-chain liquid crystal polymers with different mesogen-graft amounts has been studied by small-angle neutron scattering in dilute solutions of toluene-d8 and THF-d8. It is shown that the radius of gyration increases by about twofold when the mesogen-graft amount increases from 0 to 100%, which suggests that the persistence length of the backbone increases by about 4-fold. Comparison with the results reported in the literature on the melt state suggests that the persistence length is not an intrinsic property of side chain liquid crystal polymers, but depends on inter-chain interactions.

Keywords: Side-chain liquid crystal polymers; Persistence length; Small-angle neutron scattering

1. Introduction

In the past 15 years, the backbone conformation of side-chain liquid crystal polymers has been extensively studied, mainly using small-angle neutron scattering (SANS) after labeling the backbone by deuterium, [1–5] or X-ray diffraction [6] experiments. These studies showed an anisotropy of the backbone conformation in the oriented mesomorphic phases. This anisotropy is small in the nematic phases, and very large in the smectic phases where the backbone is essentially confined between the smectic layers. Another basic question posed by these systems concerns their persistence length l_p. A study carried out in the isotropic and unaligned nematic phases shows that the value of l_p is near that of a conventional flexible polymer [7]. This surprising result indicates that the flexibility of the chain is not modified neither by grafting the mesogenic groups every ~2.5 Å on the chain, nor by the nematic interactions. All these studies were carried out in the melt state. In order to see if this result is still valid for isolated chains, we have performed SANS experiments in dilute solutions of side-chain polysiloxanes exhibiting different mesogen-graft amounts. The results obtained show that the polymeric backbone becomes stiffer when the mesogen-graft amount is increased.

2. Experimental

2.1. Samples

The 'side-end' fixed liquid crystal polymers (LCP) investigated correspond to the chemical formula shown in Fig. 1. The precursor backbones are homohydrogenmethylsiloxanes (from Aldrich) or copolymers formed by hydrogenmethylsiloxane and dimethylsiloxane units. The copolymers were synthesized, as described elsewhere [8], in such a way that they have a similar degree of polymerization. The statistical distribution of the two types of units was checked by ^{29}Si NMR.

* Corresponding author. Tel.: +33-388-41-40-87; fax: +33-388-41-40-99.
E-mail address: guenet@ics.u-strasbg.fr (J.M. Guenet).

0032-3861/03/$ - see front matter © 2003 Published by Elsevier Science Ltd.
doi:10.1016/S0032-3861(03)00047-8

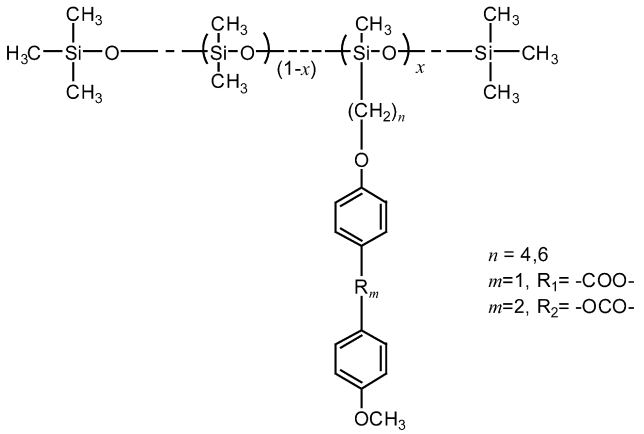

Fig. 1. Chemical formula of the side-chain LCPs under study.

Two different mesogenic groups, ended by a vinyl group, were synthesized following a procedure previously described [9]. In Fig. 1, they correspond to $n = 4$ and $m = 2$ and to $n = 6$ and $m = 1$. In the following, they will be respectively denoted P4 and P6. The side-end fixed LCP were prepared in solution by a hydrosilylation reaction between the hydrogenmethylsiloxane units and the vinyl end groups of the mesogens [10,11]. The reaction was initiated with dichloro(dicyclopentadienyl)-platinum II (500 ppm with respect to the hydrogenmethylsiloxane groups) and was carried out at 60 °C for 1 day. 1-Ethynyl-1-cyclohexanol was then introduced (1 mg/1 g of polymer) to act as a poison towards the catalyst in order to prevent from any further reaction of the possible remaining silane functions. The polymer was recovered by precipitation in methanol and purified by dissolving twice in tetrahydrofuran and precipitating again into methanol. In the following, the samples will be labeled by their mesogenic group and their mesogen-graft amount: for example, P6-85 will denote the sample having 85% ($x = 0.85$) of the monomers grafted with P6 side-groups.

The molar mass distribution of the polymers was obtained by size exclusion chromatography (SEC) in toluene coupled with light scattering (3 angles Mini Dawn; Wyatt Technology). The values of the refractive index increments used in this analysis were determined by means of a Waters 410 differential refractometer. All the polymers exhibited quite similar average number degrees of polymerization (~120), except the weakly substituted P6-8 sample. In fact, due to the low mesogen-graft amount, the precipitation of this polymer was incomplete and so favored the longest chains. The values of the molar masses and the refractive index increments are gathered in Table 1. It should be noted that, due to the low values of the refractive index increments, and to the fact that the light scattering detector has only three detector angles, the determination of the averaged molar masses lack precision.

The solutions of these side-chain LCPs were prepared in two different deutared solvents: THF-d8 and toluene-d8. Both solvents were purchased from Euriso-top and showed an isotopic enrichment ≥99.5%.

2.2. Neutron scattering

The neutron scattering experiments were carried at the Berlin Neutron Scattering Center (Hahn-Meitner-Institute Berlin) on the V4 small-angle camera. This camera is equipped with a two-dimensional sensitive detector. A sample-detector distance of 8 m was used together with a neutron wavelength of 0.6 nm (full-width at half-maximum of the wavelength distribution $\Delta\lambda/\lambda \approx 8\%$). This gives access to q values ranging from 0.07 to 0.4 nm^{-1} where $q = (4\pi/\lambda)\sin(\theta/2)$, θ being the scattering angle. Further details are available on http://www.hmi.de/bensc/instrumentation/instrumente/v4/v4.html.

The solutions were prepared directly in quartz cells from HELLMA of optical paths of 5 mm. The position sensitive detector was calibrated by means of light water, which gives off only incoherent scattering. Under these conditions the absolute intensity, $I_A(q)$ is written:

$$I_A(q) = I_N(q)/K \tag{1}$$

in which $I_N(q)$ is the intensity obtained after background subtraction, transmission corrections and detector normalization, and K is a constant, which reads:

$$K = \frac{4\pi(a_i - ya_s)^2 e_w T_w N_A}{g(\lambda_m)(1 - T_w)m_i^2} \tag{2}$$

in which a_i and a_s are the coherent scattering amplitudes of the polymer and the solvent, respectively, y is the ratio of the polymer molar volume over the solvent molar volume, T_w and e_w the transmission and the thickness of a 1 mm light water sample, m_i the molecular mass of the average scattering unit of the polymer, and $g(\lambda_m)$ a constant which is camera-dependent and was measured by using a reference sample displaying a rod-like behavior for which the mass per unit length is known (bicopper complex in *trans*-decalin [12]).

3. Results

The neutron scattering results have been analyzed by means of the Zimm approach based on the development of the scattered intensity proposed by Guinier for $qR_g < 1$, where R_g is the radius of gyration. For polydispersed systems, and under the condition that $C < C^*$, where C^* is the overlap concentration, Zimm has obtained for the reciprocal of the scattered intensity [13]:

$$\frac{C}{I_A(q)} = \frac{1}{M_w}\left[1 + \frac{q^2 R_z^2}{3}\right] + 2A_2C + 3A_3C^2 + \cdots \tag{3}$$

in which R_z^2 is the mean-square *z-averaged* radius of gyration (third moment of the distribution), M_w the *mass-*

Table 1
Characterization of the polysiloxane samples, M_n : number-averaged molar mass, M_w : mass-averaged molar mass, DP_n : number degree of polymerization, m and n refer to the chemical structure (see Fig. 1). dn/dc : refractive index increment in toluene (35 °C; 930 nm). ρ_p : polymer density as measured in toluene ($T = 25$ °C)

Sample (Pn-100x)	x	n	m	M_w (g/mol)	M_n (g/mol)	M_w/M_n	DP_n	dn/dc	ρ_p (g/cm^3)
P4-100	1	4	2	96,000	50,000	1.9	138	0.062	1.22
P6-85	0.85	6	1	14,9000	49,000	3	140	0.059	1.21
P6-50	0.5	6	1	85,000	29,000	2.9	110	0.056	1.12
P6-8	0.08	6	1	75,000	35,000	2.1	337	−0.026	1.02
Poly(hydrogen methylsiloxane)				21,000	7000	3	110	−0.078	1.01

averaged molar mass (second moment of the distribution), and A_i the virial coefficients.

As can be seen in Table 2, the values of the radius of gyration are located between 5 and 11 nm. Strictly speaking, the condition $qR_z < 1$ is not totally fulfilled in the entire investigated q-range. However, as can be seen in Figs. 2 and 3, linear Zimm-plots are obtained. This arises from the fact that the samples have polydispersities between 2 and 3, which usually allows the linear range to extend well beyond the above condition. In a few cases, the third virial coefficient had to be considered for improving the extrapolation procedure (see Fig. 3). This most probably stems from the fact that high polymer concentrations were used although still below C^* ($C^* \approx 0.2$ g/cm^3 for 0%-sample, $C^* \approx 0.1$ g/cm^3 for 100%-sample). The conspicuous invariance of the slope of the straight lines ($C/I(q)$ versus q in Figs. 3 and 4) for the three polymer concentrations used highlights the absence of concentration effect on the radius of gyration.

Table 2 shows that there is a reasonable agreement between the molar masses measured by SANS and those calculated from the neutron-determined molar mass of the poly(hydrogenmethylsiloxane). On the other hand, comparison between Tables 1 and 2 shows that the molar masses deduced from SEC are different from those measured by SANS. These discrepancies could be explained by the lack of precision of the SEC analysis discussed above. It should be stressed that these discrepancies do not question the twofold increase between the radius of gyration of the 0%-polymer and that of the 100%-sample.

4. Discussion

From Fig. 4 and from the results displayed in Table 2 it is clear that increasing the mesogen-graft amount from 0 to 100% entails an increase in the radius of gyration by a factor of nearly two. Correspondingly, the second virial coefficient decreases by approximately one order in magnitude. This means that the increase in the radius of gyration does not arise from an increase in solvent quality but is an intrinsic property of the chains.

Since the chains with the grafted mesogens cannot be considered as thin threads, the contribution of the mesogens to the measured radius of gyration should be known. This will allow one to discuss the conformation of the backbones only. By considering the presence of the mesogens as a simple thickness effect, we propose two different approaches to quantify their contribution. It should be noted here that, since the experiments were carried out in the Guinier domain, a $\ln[qI(q)]$ versus q^2 plot cannot be performed to estimate the thickness of the chains.

Table 2
Experimental values of the radius of gyration (R_z), the second virial coefficient (A_2), the third virial coefficient (A_3), the mass-averaged molar mass ($M_w^{(1)}$) as determined by SANS, the mass-averaged molar mass ($M_w^{(2)}$) as calculated from the value determined by SANS for the poly(hydrogenmethysiloxane) sample (except for the sample P6-8 because of its higher degree of polymerisation, as can be seen in Table 1). The poly(hydrogenmethysiloxane) samples used for the P6 and P4 series of experiments came from different batches

Sample (Pn-100x)	R_z (nm)	$A_2 10^4$ (cm^3/g^2)	$A_3 10^3$ (cm^6/g^3)	$M_w^{(1)}$ (g/mol)	$M_w^{(2)}$ (g/mol)
P6/deuterated toluene					
Poly(hydrogen methylsiloxane)	5.3 ± 0.5	11	0	17,000	
P6-8	8 ± 1	10	9	35,000	
P6-50	8.7 ± 1	6	1.7	58,000	63,000
P6-85	10 ± 1	4.1	0	99,000	95,500
P4/deuterated toluene					
Poly(hydrogen methylsiloxane)	5.8 ± 0.5	13	0	23,500	
P4-100	11 ± 1	0.15	0	130,000	140.000
P4/deuterated THF					
Poly(hydrogen methylsiloxane)	5.8 ± 0.5	15	0	23,000	
P4-100	9 ± 1	1.1	0.55	128,000	137,000

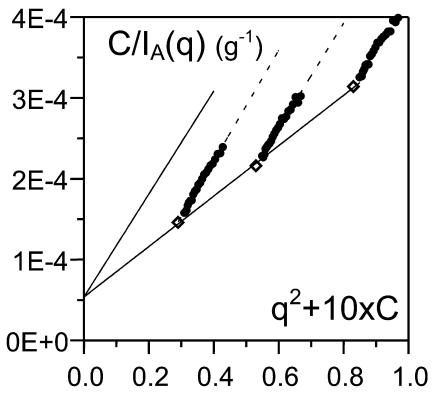

Fig. 2. Zimm-plot for 0%-sample in THF; $C_{pol} = 0.083$, 0.055, 0.029 g/cm^3. The open symbols stand for the extrapolation at $q = 0$ nm^{-1}.

In the first approach, it is assumed that the average of a system of chains with hanging side-groups is a chain with a circular cross-section. As demonstrated in Appendix A, R_n^2, the mean-square *n-average* of the radius of gyration of the system of chains can then be written:

$$R_n^2 = R_{nb}^2 + R_c^2 \tag{4}$$

where R_{nb}^2 is the mean-square *n*-average of the radius of gyration of the backbone and R_c^2 the squared radius of gyration of the cross-section, which show no polydispersity.

The second approach is based on a decomposition of the intensity $i(q)$ scattered by one chain [14,15]:

$$i(q) = i_b(q)\Phi(q) \tag{5}$$

where $i_b(q)$ is related to the backbone of the chain and $\Phi(q)$ to its cross-section. With R_g the global radius of gyration and R_{gb} the radius of gyration of the backbone, the Guinier's development of the intensities gives $i(q) \propto e^{-q^2R_g^2/3}$ and $i_b(q) \propto e^{-q^2R_{gb}^2/3}$. A Guinier development for the cross-section [15,16] gives: $\Phi(q) \propto e^{-q^2R_c^2/2}$, with R_c the radius of gyration of the cross-section, as previously. The following expression can then be deduced from Eq. (5):

$$R_g^2 = R_{gb}^2 + \frac{3}{2}R_c^2 \tag{6}$$

For many-chains systems, average parameters should be

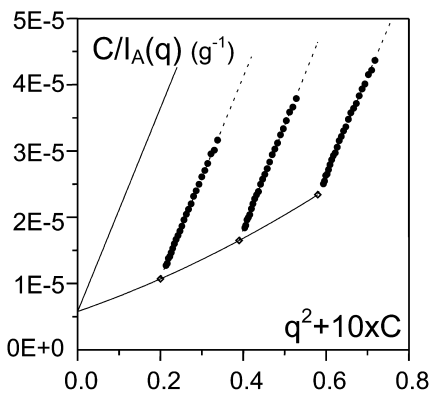

Fig. 3. Zimm-plot for 100%-sample in THF; $C_{pol} = 0.058$, 0.039, 0.02 g/cm^3. The open symbols stand for the extrapolation at $q = 0$ nm^{-1}.

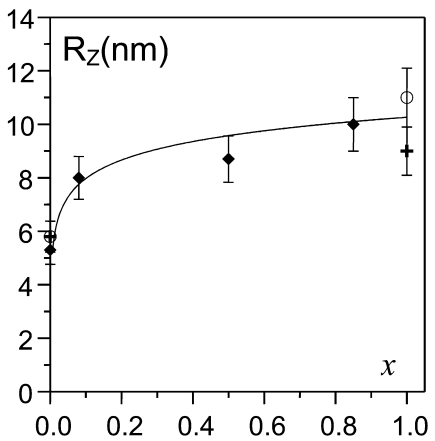

Fig. 4. Variation of the radius of gyration as a function of the mesogen-graft amount x. (◆) = P6 samples in toluene, (○) = P4 in toluene, (+) = P4 in THF. The solid line is a guide for the eyes.

introduced. R_g^2 and R_{gb}^2 in Eq. (6) can be replaced by R_n^2 and R_{nb}^2, respectively: these parameters are independent of the polydispersity and can therefore be compared to the cross-sectional radius of gyration. One can note that Eq. (6) differs from Eq. (4) by the 3/2 factor of the R_c^2 term. This discrepancy comes from the fact that the two approaches are based on different approximations, which lead to approximate expressions. However, as this will clearly appear below, this point has no incidence on the fact that the R_c^2 term is negligible compared to the R_{gb}^2 term.

Since the systems under study are polydisperse, the scattering experiments give access to the mean-square *z*-average of the global radius of gyration, namely R_z^2. In order to deduce the R_n^2 values from the measured R_z^2 values, the molar mass distribution is approximated by a distribution function. For that purpose, it is convenient to choose the widely used Schulz-distribution function [17]. It is defined as followed:

$$w(M) = \frac{M^{1/U}}{\Gamma\left(1+\frac{1}{U}\right)\left(\frac{M_w}{1+\frac{1}{U}}\right)^{1+1/U}} \exp\left(-\frac{M}{M_w}\left(1+\frac{1}{U}\right)\right) \tag{7}$$

where Γ represents the gamma function, M is the continuous variable for the molar mass and $U = I - 1$ if I is the polydispersity (values of $I = M_w/M_n$ are listed in Table 1). $w(M)$ is defined for a discrete system of N_i chains of molar mass M_i by: $w(M_i) = N_iM_i/\sum N_iM_i$. R_n^2 and R_z^2 can be then defined in gaussian approximation by [18]:

$$R_z^2 = (1+2U)R_n^2 \tag{8}$$

The use of a relation suitable for gaussian chains, whereas the chains under study are not gaussian, has no incidence on our discussion and will be justified later when discussing the

determination of the persistence length. From Eq. (8), it appears that the calculated values of R_n^2 for the partially or totally substituted samples are included in the range:

$$16 \leq R_n^2 \leq 44 \text{ nm}^2 \quad (9)$$

For a fully substituted chain, R_c^2 can be estimated by considering that the side groups are rods of length $d \approx 2.5$ nm and radius $b \approx 0.2$ nm, and is given by [19]:

$$R_c^2 = \frac{d^2}{12} + \frac{b^2}{2}$$

Since the thickness effect due to the side groups is less important for a partially substituted chain than for a fully substituted one, the present estimation will lead to a maximal value for the R_c^2 term of Eqs. (4) and (6). The calculation gives $R_c^2 \approx 0.6$ nm^2. Comparing this value to those of R_n^2 deduced from relationship (9), it appears clearly that the main term in Eqs. (4) and (6) is R_{nb}^2. Thus, we have shown that the quantity measured by SANS reflects actually the radius of gyration of the backbone of the polymer. This result stems from the fact that the length of the side groups, $d \approx 2.5$ nm, is much smaller than the average contour length of the chains, which is higher than 30 nm. We will now compare the standard polymer and the liquid crystal polymer under study in terms of the rigidity of their backbone.

An increase in the rigidity of the chains when grafting side-groups is qualitatively obvious: the experimental data in Tables 1 and 2 show that the radius of gyration is increasing when the degree of polymerization remains approximately the same (except for the sample P6-8 because of its incomplete precipitation, as explained previously). A more quantitative approach can be given by the determination of the persistence length of the side-chain liquid crystal polymers, which, in first approximation, is the backbone one.

In the frame of persistence length chain model, Benoît and Doty [20] have established the following equation between the radius of gyration R_g, the contour length L of the finite chain and the persistence length l_p :

$$R_g^2 = \frac{Ll_p}{3} - l_p^2 + \frac{2l_p^3}{L} - \frac{2l_p^4}{L^2}(1 - e^{-L/l_p}) \quad (10)$$

In the case of polymers in solution, this relation is valid for unperturbed chains, i.e. for polymer–solvent systems at the Θ temperature. Above this temperature, in 'good solvent', excluded volume effects occur, the chains swell and the second virial coefficient A_2 becomes positive. Is it therefore possible to employ Eq. (10) for the systems under study? A priori the answer is no since the measured values of A_2 (Table 2) are positives. However, the value of l_p determined with Eq. (11) (see Table 3 and the following text) for the non-substituted chain, $l_p = 0.5$–0.6 nm, is very close to the persistence length $l_p = 0.54$ nm reported in the literature [21] for an ordinary poly(dimethylsiloxane) chain. Assuming that the flexibilities of poly(dimethylsiloxane) and poly(hydrogenmethysiloxane) are identical, this agreement indicates that Eq. (10) can be used for the non-substituted chains under study, despite the positive value of A_2. Moreover, excluded volume effects decrease for the substituted chain, as shown by the lower values of A_2 : it is then reasonable to use Eq. (10) for all the samples. This result can be understood as being a consequence of the low molecular mass of the chains, i.e. their low conformational entropy.

Table 3
Calculated values of the persistence length (l_p), using Eq. (11) and with the experimental values of the radius of gyration R_z, the contour length L_w and the polydispersities I

Sample (Pn-100x)	R_z (nm)	L_w (nm)	$U = I - 1$	l_p (nm)
P6/deuterated toluene				
Poly(hydrogen methylsiloxane)	5.3 ± 0.5	85	2	0.6
P6-8	8.0 ± 1	106	1.1	1.2
P6-50	8.7 ± 1	76	1.9	1.9
P6-85	10.0 ± 1	88	2	2.1
P4/deuterated toluene				
Poly(hydrogen methylsiloxane)	5.8 ± 0.5	118	2	0.5
P4-100	11.0 ± 1	109	0.9	2.4
P4/deuterated THF				
Poly(hydrogen methylsiloxane)	5.8 ± 0.5	115	2	0.5
P4-100	9.0 ± 1	107	0.9	1.6

Eq. (10) should be now adapted for the quantities which are experimentally accessible. By using the Schulz distribution of the molar masses, Oberthür [18] has obtained:

$$R_z^2 = \frac{1+2U}{1+U}\frac{L_w l_p}{3}\left(1 - \frac{1+U}{1+2U}\frac{3l_p}{L_w}\left(1 - \frac{2l_p}{L_w}\right) - \frac{(1+U)^2}{1+2U}\frac{6l_p^3}{L_w^3}\left[1 - \left(1 + \frac{U}{1+U}\frac{L_w}{l_p}\right)^{-\frac{1}{U}}\right]\right) \quad (11)$$

where the contour length L_w is defined by $L_w = (l/\tilde{m})M_w$, M_w being the mass-average molar mass of the chains, l the distance between repetitive units and $\tilde{m}$ the molar mass of a monomer unit (for partially substituted chains, $\tilde{m}$ is the average mass of a monometer unit). M_w is measured by SANS (see Table 2), l is about 0.3 nm for a polysiloxane and $\tilde{m}$ is known for each sample, so L_w can be deduced for each sample. With the experimental values of R_z (Table 2), the values of l_p can be obtained by a numerical resolution of Eq. (11). These values are gathered in Table 3.

Table 3 shows that the increase in the persistence length is observed in the two solvents and for the two different mesogens considered. The discrepancy between the results for the two sets of experiments (with P4 or P6 side-groups) stems from the fact that the poly(hydrogenmethysiloxane)

used are issued from different chemical synthesis. It can be seen that the persistence lengths calculated for poly(hydrogenmethylsiloxane) of the two syntheses are identical considering an accuracy of 0.1 nm. Finally, it is clearly shown in Table 3 that the persistence length of the polymer backbones increases by a factor ranging from 3 to 5, from the starting polymer to the fully substituted one. It is clear that the numerical evaluation of l_p depends on the choice of the molar masses distribution. The present estimations, obtained with the Schulz distribution, seem to be correct since they give a value compatible to the literature for the persistence length of the non-substituted chain. The results shown in Table 3 also indicate that a small mesogen-graft amount already produces a marked effect on the persistence length. To quantify the increase in persistence length, a larger number of monomers should be used in the simulation: this is outside the scope of this paper.

Finally, it should be noted that an increase in the persistence length has been suggested by Fredrickson on the basis of theoretical calculations carried out by considering a model system where the side groups and the backbone are of identical chemical structure [22]. These analytical predictions were later confirmed by Saariaho et al. [23] by means of Monte-Carlo simulations. Fredrickson's calculations are not directly tractable under the present conditions as we are dealing here with a polymer of disparate moieties.

5. Concluding remarks

The experimental determination of R_z points towards an increase of the backbone's persistence length with increasing the mesogen-graft amount in the dilute state. Recent results reported by Fourmaux-Demanges et al. [7] in the isotropic and nematic melt-state have shown that the persistence length is about 1 nm for liquid crystal polymers made of poly(methylmethacrylate) with mesogen-graft amounts of 100%. Since the persistence length for the standard poly(methylmethacrylate) is about 0.7 nm [24], the presence of the mesogens does not modify significantly the rigidity of the chain in the melt state. Since the increase in the persistence length in solution is clearly a consequence of intra-chain interactions, the comparison between these results and those in the melt state suggests that a balance between intra and inter-chain interactions is responsible of the unchanged value of l_p in the melt state. The persistence length is therefore not an intrinsic property of side-chains liquid crystal polymers.

Acknowledgements

It is a pleasure to thank L. Noirez for many stimulating discussions and helpful remarks about the analysis of the data. The experiments at BENSC in Berlin were supported by the European Commission under the Access to Research Infrastructures Action of the Human Potential Programme (contract: HPRI-CT-1999-00020).

Appendix A. Mean-square *n*-average radius of gyration of a system of chains with hanging side-groups (demonstration of Eq. (4))

The following calculation is based on the method proposed by Reinecke et al. in Ref. [25]. The square radius of gyration of a single chain is written:

$$R_p^2 = \frac{1}{2N^2}\sum_{i,j} A_i A_j^2 \tag{A1}$$

in which $A_iA_j^2$ stands for the square distance between any two points in the chain, N being the number of these points. The vector $\mathbf{A}_i\mathbf{A}_j$ can be expressed through (see Fig. 5):

$$\mathbf{A}_i\mathbf{A}_j = \mathbf{A}_i\mathbf{O}_m + \mathbf{O}_m\mathbf{O}_n + \mathbf{O}_n\mathbf{A}_j \tag{A2}$$

in which O_m and O_n are the intersections between the backbone of the chains and the cross-sectional areas perpendicular to the backbone. Squaring Eq. (A2) gives:

$$A_iA_j^2 = A_iO_m^2 + O_mO_n^2 + O_nA_j^2 + 2\mathbf{A}_i\mathbf{O}_m\cdot\mathbf{O}_m\mathbf{O}_n + 2\mathbf{O}_n \mathbf{A}_j\cdot\mathbf{O}_m\mathbf{O}_n + 2\mathbf{A}_i\mathbf{O}_m\cdot\mathbf{O}_n\mathbf{A}_j \tag{A3}$$

with N_L the number of cross-sectional areas and n_c the number of scatterers per cross-sectional area, the mean-square n-average radius of gyration of a system of chains is

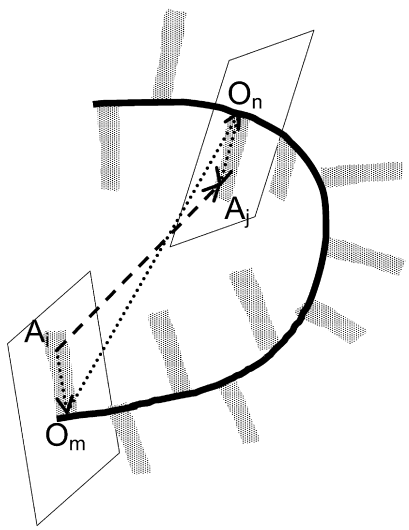

Fig. 5. Schematic drawing of a part of a chain with hanging side-groups. Vector $\mathbf{A}_i\mathbf{A}_j$ is shown to be the sum of three vectors, namely $\mathbf{A}_i\mathbf{O}_m + \mathbf{O}_m\mathbf{O}_n + \mathbf{O}_n\mathbf{A}_j$, where O_m and O_n are the intersections between the backbone of the chains and the cross-sectional areas perpendicular to the backbone.

then written:

$$R_n^2 = \frac{\sum\left[\frac{1}{2N_L^2 n_c^2}\sum_{n,m,i,j}(A_i O_m^2 + O_m O_n^2 + O_n A_j^2 + 2\mathbf{A}_i \mathrm{O}_m \cdot \mathbf{O}_m \mathbf{O}_n + 2\mathbf{O}_n \mathbf{A}_j \cdot \mathbf{O}_m \mathbf{O}_n + 2\mathbf{A}_i \mathbf{O}_m \cdot \mathbf{O}_n \mathbf{A}_j)\right]}{\sum N_p} \tag{A4}$$

where the main summation $\sum$ extends to all the chains in the system, N_p being the number of chains with radius of gyration R_p.

Due to the averaging on all the chains of the system, any vector $\mathbf{A}_i\mathbf{O}_m$ and $\mathbf{A}_j\mathbf{O}_n$ possess an opposite counterpart, so that cross-terms in Eq. (A4) cancel by pair when the summation over all possible values of $A_i A_j^2$ is performed. Eq. (A4) becomes:

$$R_n^2 = \frac{\sum\left[\frac{1}{2N_L^2 n_c^2}\sum_{m,n,i,j} O_m O_n^2 + \frac{1}{2N_L^2 n_c^2}\sum_{m,n,i,j} A_i O_m^2 + \frac{1}{2N_L^2 n_c^2}\sum_{m,n,i,j} O_n A_j^2\right]}{\sum N_p} \tag{A5}$$

which can eventually be written:

$$R_n^2 = \frac{\sum\left[\frac{1}{2N_L^2}\sum_{m,n} O_m O_n^2\right]}{\sum N_p} + \left[\frac{1}{2n_c}\sum_i A_i O_m^2 + \frac{1}{2n_c}\sum_j O_n A_j^2\right] \tag{A6}$$

The first term is the mean-square *n*-average of the radius of gyration of the backbone, while the last term yields to the radius of gyration of the cross-section.

References

[1] Kirste RG, Ohm HG. Makromol Chem Rapid Commun 1985;6:179.
[2] Keller P, Carvalho B, Cotton JP, Lambert M, Moussa F, Pépy G. J Phys Lett 1985;46(L):1065.
[3] Moussa F, Cotton JP, Hardouin F, Keller P, Lambert M, Pépy G, Mauzac M, Richard H. J Phys 1987;48:1079.
[4] Noirez L, Cotton JP, Hardouin F, Keller P, Moussa F, Pépy G, Strazielle C. Macromolecules 1988;21:2891.
[5] Le Commandoux S, Noirez L, Mauzac M, Hardouin F. J Phys II (France) 1994;4:2249.
[6] Davidson P, Levelut AM. Liq Cryst 1992;11:469.
[7] Fourmaux-Demange V, Boué F, Brûlet A, Keller P, Cotton JP. Macromolecules 1998;31:801.
[8] Leroux N, Mauzac M, Noirez L, Hardouin F. Liq Cryst 1994;3:421.
[9] Marty J-D, Tizra M, Mauzac M, Rico-Lattes I, Lattes A. Macromolecules 1999;32:8674.
[10] Degert C, Richard H, Mauzac M. Mol Cryst Liq Cryst 1992;214:179.
[11] Gallani J-L, Hilliou L, Martinoty P, Doublet F, Mauzac M. J Phys II (Paris) 1996;6:443.
[12] Lopez D, Guenet JM. EPJ B 1999;B12:405.
[13] Zimm BH. J Chem Phys 1948;16:1099.
[14] Rawiso M, Aime J, Fave J, Schott M, Müller M, Schmidt M, Baumgartl H, Wegner G. J Phys (France) 1988;49:861.
[15] Koyama RJ. Phys Soc Jpn 1974;36:1409.
[16] Porod G. In: Glatter O, Kratky O, editors. Small angle X-ray scattering. New York: Academic Press; 1982. p. 32–5.
[17] Schulz GV. Z Phys Chem 1939;43(Abt B):25.
[18] Oberthür RC. Makromol Chem 1978;179:2693.
[19] Higgins J, Benoît H. Polymers and neutrons scattering. Oxford: Clarendon Press; 1994.
[20] Benoît H, Doty P. J Phys Chem 1953;87:858.
[21] Schulz G, Haug A. Z Phys Chem (Frankfurt) 1962;34:328.
[22] Fredrickson GH. Macromolecules 1993;26:2825.
[23] Saariaho M, Ikkala O, Szleifer I, Erukhimovich I, ten Brinke G. J Phys Chem 1997;107:3267.
[24] Kirste R, Kratky OZ. Phys Chem (Frankfurt) 1962;31:363.
[25] Reinecke H, Mijangos C, Lopez D, Guenet JM. Macromolecules 2000;33:2049.